P4.7 USE/IMPACT OF NESDIS GOES WIND DATA WITHIN AN OPERATIONAL MESOSCALE FDDA SYSTEM

Jennifer M. Cram[1*], Jaime Daniels[2], Wayne Bresky[3], Yubao Liu[1], Simon Low-Nam[1], Rong-Shyang Sheu[1]
[1]NCAR/RAP, Boulder, Colorado
[2]NOAA/NESDIS, Camp Springs, Maryland
[3]Raytheon Information Technology & Scientific Services (ITSS), Lanham, Maryland

1. INTRODUCTION

A mesoscale, real-time, four-dimensional data assimilation (RT-FDDA) and short-term forecasting system has been developed for the U.S. Army Test and Evaluation Command (ATEC) at the Dugway Proving Ground (DPG) in Utah. This MM5-based analysis and forecast system (Cram et al., 2001) provides a continuous series of updated 3-dimensional analyses and a new 12-hr forecast on 3 domains (30 km, 10km, and 3.3 km grid spacings) every 3 hours in real-time. The system uses many diverse data sets available over the region: standard surface and upper air observations, special surface observations, the University of Utah Mesowest observations (extensive western U.S. mesonet), DPG local surface observations, DPG profilers and RASS instrumentation, and NESDIS GOES wind vectors. The NESDIS GOES wind vectors are a unique data set in that their horizontal and vertical locations are never pre-determined, and there is always a very uneven distribution - ranging from dense coverage in some local regions to no coverage in other regions. The impact of the GOES wind data is measured by comparing parallel versions of the RT-FDDA system, with and without the NESDIS data set, with the systems' error calculated against the standard rawinsonde data set.

2. RT-FDDA SYSTEM DESCRIPTION

The RT-FDDA system uses a unique cycling methodology which provides the end-user with a continuous series of updated 3-dimensional analyses and a new 12-hr forecast on 3 domains (30 km, 10km, and 3.3 km grid spacings) every 3 h in real-time. The multi-stage cycling methodology is designed to take best advantage of the differing data ingest lags encountered in a real-time system (valid time lags can range from only a few minutes to 2 h), and uses a model-restart capability to provide continuous, balanced, 3-dimensional analyses and forecasts at any time interval. Fig. 1 illustrates the cycling methodology.
The data assimilation method is Newtonian relaxation (nudging) in the Pennsylvania State University (PSU)/NCAR MM5 Version 4 (Grell et al., 1995) model, which allows for a time-continuous system and use of observational data at all times (not just on-the-hour). On small scales we want to allow for model development in data sparse regions, but we want to adjust to observations where they exist; the choice of Newtonian relaxation allows this. The FDDA system runs continuously and assimilates data continuously. Each

Corresponding author address: Jennifer M. Cram, NCAR/RAP, P.O. Box 3000, Boulder, CO 80307-3000; email: cram@ucar.edu

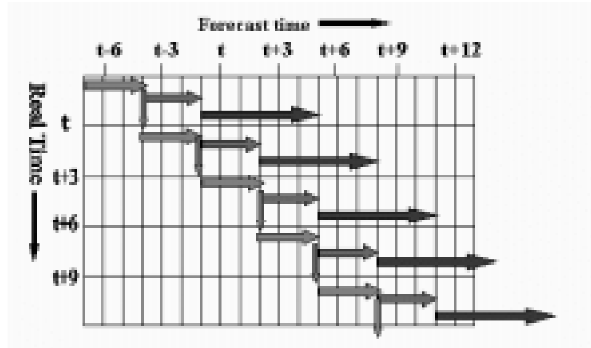

Fig. 1. Cycle diagram for the RT-FDDA system. Every 3 hours,: a) (lightest gray) final FDDA nudging stage, from t-4 to t-1. This stage is initialized as a re-start from the previous cycle's final FDDA stage; b) (in medium gray) preliminary FDDA nudging cycle from t-1 to t+2 - use all data ingested to that point.and restarts from final cycle analysis at t-1; c) (in darkest gray) forecast from t+2 onwards.

new model cycle is a restart from the previous final FDDA cycle analyses; no extra time is therefore needed for cloud or precipitation spin-up, and the model atmosphere is continuously evolving. The RT-FDDA system is described more thoroughly in Cram et al. (2001).

3. MODEL CONFIGURATION AND SPECIFICS

The PSU/NCAR MM5 model is used as the basis of this data assimilation system. The FDDA system runs on 3 interactive grids centered over the western U.S. (Fig. 2), with grid spacings ranging from 30 km down to 3.3 km. The basic MM5 model configuration used in the RT-FDDA system is summarized as:

- Non-hydrostatic
- Interactive nesting procedure
- Radiative top boundary condition
- Time-changing lateral boundary conditions
- Grell cumulus parameterization on 10+ km grids.
- Simple ice explicit moisture scheme
- MRF (or Hong-Pan) PBL scheme
- Cloud radiation scheme
- Multi-layer soil temperature model.
- Simple soil moisture variability bucket scheme
- Snow fall/melt scheme (Low-Nam et al., 2001)

Newtonian Relaxation (nudging) of observations (vs. analysis nudging) is used to assimilate the observations into the MM5 model. The FDDA Newtonian relaxation algorithm as implemented in the MM5 model is documented in Grell et al. (1995). Although many of the concepts and algorithms from the standard MM5 nudging software were retained, the

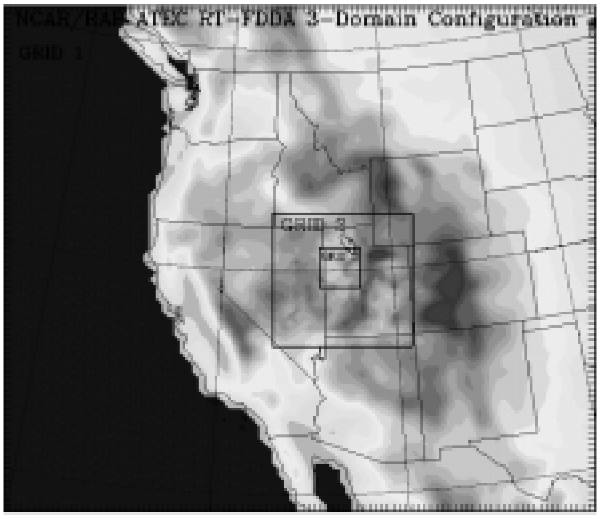

Fig. 2. The current 3-domain configuration used for the NCAR/RAP ATEC RT-FDDA system. Grid 1 has a 30 km horizontal spacing with 96*84 grid points. Grid 2 has a 10 km horizontal spacing with 70*67 grid points. Grid 3 has a 3.3 km horizontal spacing with 61*61 grid points.

observation nudging routines were substantially re-written for this RT-FDDA system and some of the concepts only available to the analysis nudging routines in the standard MM5 release were adapted to apply to the observation nudging routines. The nudging parameters and algorithms used in this RT-FDDA system are described most thoroughly in Cram et al. (2001). Parameters especially applicable to this satellite wind data study are described below.

The nudging factor is set to 6.E-4s^{-1} for all variables (u,v,T,q) and is equivalent to a forcing time scale of approximately 30 minutes. The maximum horizontal radius varies with domain : R=240 km on grid 1, 120 km on grid 2, and 80 km on grid 3. The time window is +/- 40 minutes around observation valid time.

For a single-point upper air observation (satellite wind observations), $w_z = 1 - \left| p_{obs} - p_{ijk} \right| / R_p$. When $\left| p_{obs} - p_{ijk} \right| \le R_p$, R_p is the vertical radius of influence, set to 75 mb. $w_z = 0$, when $\left| p_{obs} - p_{ijk} \right| > R_p$

The continuous assimilation method allows the use of observations at all times, not just those clustered around the 12-hourly, 3-hourly, or even hourly times. The University of Utah coordinates the compilation of observations from close to 20 different networks in the western US, many with observation frequencies of 15 minutes or less (Horel et al., 2000) , and all of those observations are incorporated into this system, along with standard WMO observations (surface, upper air, and asynoptic specials). Also, since this system was developed for an ATEC range there is a local automated surface mesonet on the range with observations at 15 min periods, and local profilers and RASS instrumentation with observations available at 20 min intervals. Satellite-derived wind information available from NESDIS (Gray et al., 1996; Nieman et al., 1997) is also incorporated into the system. Table 1 shows the typical surface data availability within +/- 40 minutes around the top of the hour on all 3 grids.

The quality control software performs gross error checks, buddy checks, and checks against a first-guess as defined by the previous cycle's preliminary and forecast stages. The WMO data sets, Utah Mesowest data sets, NESDIS satellite winds, and ATEC range surface mesonet data sets are processed with this quality control. The range profiler and RASS data sets have their own quality control thresholds.

Obs Totals	**Grid 1**	**Grid2**	**Grid3**
Metars	468	42	5
Special	207	23	1
Ship	29	0	0
U of Utah	2799	859	296
Temp	1	0	0
Pilot	2	0	0
Sat-wind	731	45	0
SAMS	95	95	95
Profilers	0	0	0

Table 1: Observation totals for the +- 40 min period around 2001040617 in the final stage.

4. THE SATELLITE WIND DATA SETS

The Geostationary Operational Environmental Satellite (GOES) cloud-drift winds and water vapor (WV) motion winds used in this study were provided by the National Oceanic and Atmospheric Administration (NOAA)/ National Environmental Satellite Data and Information Service (NESDIS). The GOES satellites observe the earth with an imaging radiometer. For the derivation of winds, three channels on the GOES satellites are used. These include the visible channel (0.65um), the infrared (IR) window channel (11.4um), and the WV channel (6.7um) with a horizontal resolution (at nadir) of 1km, 4km, and 8km respectively.

The satellite wind products are generated in an automated operational environment at NOAA/NESDIS and are made available to the numerical weather prediction (NWP) community for use in both regional and global atmospheric models. The cloud-drift and WV winds are complimentary in nature. Cloud-drift winds are derived primarily in cloudy and partly cloudy areas, while the largest percentage of the WV winds are generated in cloud-free areas. Table 2 illustrates the frequency at which each product is produced, together with the GOES image sector and image time interval used.

The satellite wind products are derived using a sequence of three images with a temporal resolution shown in this table. The winds are derived using a three-step objective procedure which is described in more detail in Nieman et al. (1997). The initial step involves selecting valid tracers in the middle image where local gradients in brightness are computed for each pixel in the target domain. The pixel with the largest gradient is chosen as the target. The next step in the process involves assigning representative heights to each of these tracers. For opaque cloud tracers, a histogram of IR window channel brightness temperatures is used, together with a coincident forecast temperature profile (from a short-term global aviation model forecast obtained from the National Center for Environmental Prediction (NCEP)/Environmental Modeling Center (EMC)), to assign a pressure height. For optically thin cirrus tracers, a multi-spectral technique which entails utilization of both the IR window and WV imagery (Schmetz and Holmlund, 1992) is used. For water vapor tracers in cloud-free environments, the mean WV brightness temperature centered over the target is used together with a coincident short-term aviation model forecast temperature profile to assign a pressure height. The next step involves tracking the identified tracers both backward (using the second and first images) and forward (using the second and third images) in time. Two displacement vectors are computed which are then compared for consistency; wind vector pairs which are not consistent are eliminated. Once all of the wind vectors have been computed, an automated objective quality control procedure (Hayden and Velden, 1991) is invoked. A three-dimensional objective analysis (Hayden and Purser, 1995) of the satellite wind field, again using background information from the NCEP/EMC global aviation NWP prediction model, is performed. Tracer height assignments are evaluated during this step, and in some cases, adjusted. Finally, an objective re-analysis using all wind vectors (those passing quality control tests and those whose heights have been readjusted) is performed where the preliminary analysis is used as the background. This allows for the assignment of quality flags to the satellite winds.

5. SATELLITE DATA SENSITIVITY TESTS

Satellite wind data sets have been available in real-time from NESDIS (via ftp) at approximately 3 hr intervals. An example of the total observation counts available to each grid within the fdda system at one particular time (2001040617) is shown in Table 1. Figs. 3a-c show the wind vectors valid at that time exactly, plotted in 3 different layers.

Sensitivity tests between 2 parallel versions of the RT-FDDA system were performed for 3 consecutive weeks in April 2001 - statistics from only the first week are shown but are consistent with those from the other 2 weeks. One version of the system used all available data (denoted SAT) and the second version used all available data except the satellite wind observations (NOSAT). Verification statistics were calculated for both versions against the rawinsonde observations. These statistics were calculated for all cycles and stages that had a valid time at a synoptic time – these cycles and stages are summarized in Table 3. The satellite wind total observation count for 1-7 April 2001 (within the RT-FDDA system domain) is shown in Fig 4. The maxima in observation availability occur at 300 and 900 hPa. The calculated mean absolute error (MAE) wind

Winds Product	***Frequency (Hours)***	***Image Sector(s)***	***Image Interval (Min)***
IR Cloud-drift	3	RSOP	7.5
	3	PACUS/ CONUS	15
	3	Extended NH; SH	30
Vis Cloud-drift	3	RSOP	7.5
	3	PACUS/ CONUS	15
	3	Extended NH; SH	30
Water Vap (Cloud-top)	3	Extended NH; SH	60
Water Vap (Clear-air)	3	Extended NH;SH	60

Table 2: NOAA/NESDIS GOES Satellite Wind Products (RSOP - Rapid Scan Operations; PACUS - Pacific US; CONUS - Continental US)

Cycle	**Stage**	**Valid at**
02 UTC	Final	00 UTC
14 UTC	Final	12 UTC
23 UTC	Prelim	00 UTC
11 UTC	Prelim	12 UTC
20 UTC	Fcst02	00 UTC
08 UTC	Fcst02	12 UTC
17 UTC	Fcst05	00 UTC
05 UTC	Fcst05	12 UTC

Table 3: Cycles and Stages used in the verification. These particular cycle/stage combinations are the ones that have valid times coinciding with synoptic times.

speed statistics for the SAT and NOSAT FDDA systems over the period from 2001040100 through 2001040712 are shown in Fig. 5. The SAT system shows a small but consistent improvement over the NOSAT system. Note that the greatest improvement in Fig. 5 corresponds to the levels of maximum observation counts. The satellite wind observations are always included in the final stage assimilation (data cutoff window 1-4 hrs previous), and often make it into the preliminary stages too (data cutoff window from 0-2 hrs). There is no data assimilation included at all in the forecast stages. The rawinsondes against which the systems are verified are included in the assimilation system; because of their timing the rawinsondes only make it into the final stage assimilations.

6. SUMMARY

A simple sensitivity test was performed to test the impact of the NOAA/NESDIS satellite wind vector product as used in an operational, mesoscale RT-FDDA system. The results indicate a small but consisten t positive impact on the system when the

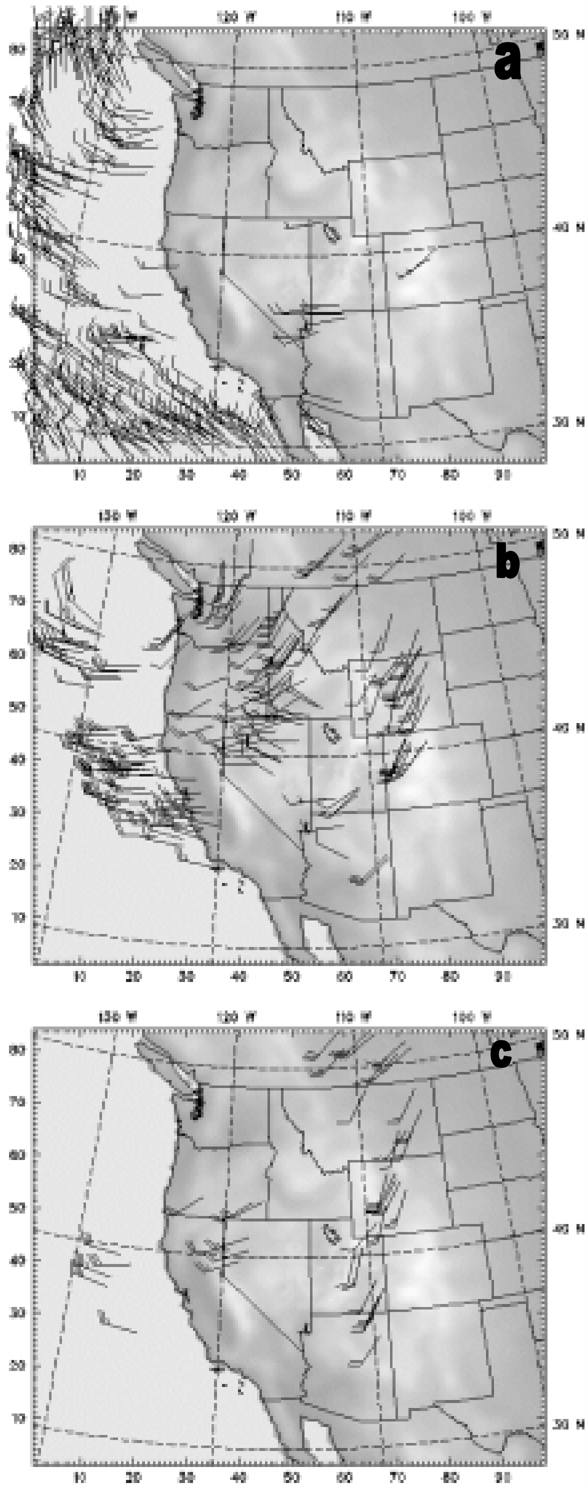

Fig. 3. Wind vectors valid at 2001040617 and within domain 1 , plotted in 3 different layers: a) surface to 600 hPa, b) 600 to 350 hPa, and c) 350 to 50 hPa.

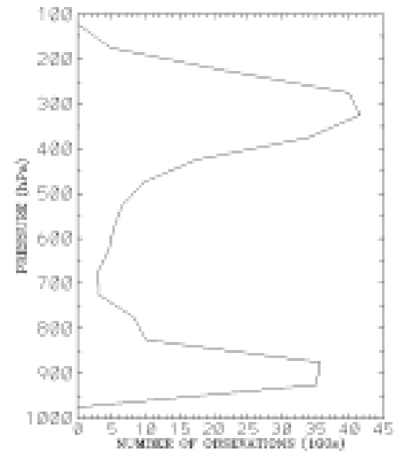

Fig. 4. Total count of all satellite wind observations within the FDDA domain for the period from 2001040100 through 2001040712, classified by level.

NESDIS wind data sets are used. Many questions remain unanswered however:

- Will the impact be improved with the usage of more frequent (hourly) satellite wind data sets?
- What is the effect of grid spacing on the impact? The RT-FDDA system currently assimilated the wind vectors as available on all 3 grids – 30 km, 10 km, and 3.3 km grid spacings. Given that the satellite wind vectors have an inherent individual coverage of 30-60 km (each vector is determined from a 15*15 pixel box, and the pixel size varies between the visible, IR, and WV imageries), perhaps the assimilation should only occur on the 30 km model grid?
- Should the Newtonian relaxation weights vary with grid (i.e. with the model resolution)? Should the vertical weighting function be adjusted, perhaps dependent on vertical wind shear? Should the horizontal weighting function be anisotropic, (Benjamin and Seaman, 1985)?
- Should the Newtonian relaxation weights vary with imagery type (perhaps a weighting dependent upon reliability or accuracy)? The horizontal, vertical, and timing weight parameters can all vary with observation type, as well as the main nudging parameter. Although the ability to vary the weights with platform type is built into the system, we have not yet experimented with varying the weights with platform type.
- What is the impact of the satellite wind assimilation on other variables? Could the impact be improved if a balance constraint was applied to simultaneously adjust the mass fields? Should such a constraint only be applied on the domains with grid spacings above some limit (20 km for example, to differentiate synoptic and mesoscale resolutions)?

7. REFERENCES

Benjamin, S.J., and N.L. Seaman, 1985: A simple scheme for objective analysis in curved flow. *Mon. Wea. Rev.*, 113, 1184-1198.

Cram, J.M., Y. Liu, S. Low-Nam, R-S. Sheu, L. Carson, C.A. Davis, T. Warner, J.F. Bowers, 2001: An operational mesoscale RT-FDDA analysis and forecasting system. *Preprints 18th WAF and 14th NWP Confs*., Ft. Lauderdale, AMS, Boston, MA. 5 pp.

Gray, D. J. Daniels, S. Nieman, S. Lord, and G. Dimego, 1996: NESDIS and NWS Assessment of of GOES 8/9 Operational satellite motion vectors. *Proceedings 3rd Int. Winds Workshop, Ascona, Switzerland*. EUMETSAT Pub. EUM P18, ISSN 1023-0416, p175-183.

Grell, G.A., J. Dudhia, and D.R. Stauffer, 1995: A description of the Fifth-generation Penn State/NCAR Mesoscale Model (MM5). NCAR/TN-398, NCAR, Boulder, CO. 122 pp.

Hayden C.M., and R.J. Purser, 1995: Recursive filter objective analysis of meteorological fields, applications to NESDIS operational processing. *J. Appl. Meteor*, **34**, 3-15.

Horel, J., M. Splitt, B. White, 2000: Mesowest: Cooperative mesonets in the western United States. *Preprints 14th Symposium on Boundary Layer and Turbulence*, 7-11 August 2000, Aspen, CO. AMS, Boston, MA. 414-417.

Low-Nam, S., C.A. Davis, J.M. Cram, Y. Liu, and R.-S. Sheu, 2001: Use of a snow prediction scheme in a mesoscale real-time FDDA system. *Preprints 18th WAF and 14th NWP Confs*., Ft. Lauderdale, AMS, Boston, MA. 5 pp.

Nieman, S.J., W.P. Menzel, C.M. Hayden, D. Gray, S. Wanzong, C. Velden, and J. Daniels, 1997: Fully automated cloud-drift winds in NESDIS operations. *Bull. Amer. Meteor. Soc.*, **78**, 1121-1133.

Schmetz, J., and K. Holmlund, 1992: Operational cloud motion winds from Meteosat and the use of cirrus clouds as tracers. *Adv. Space Res.*, **12**, No. 7, 95-104.

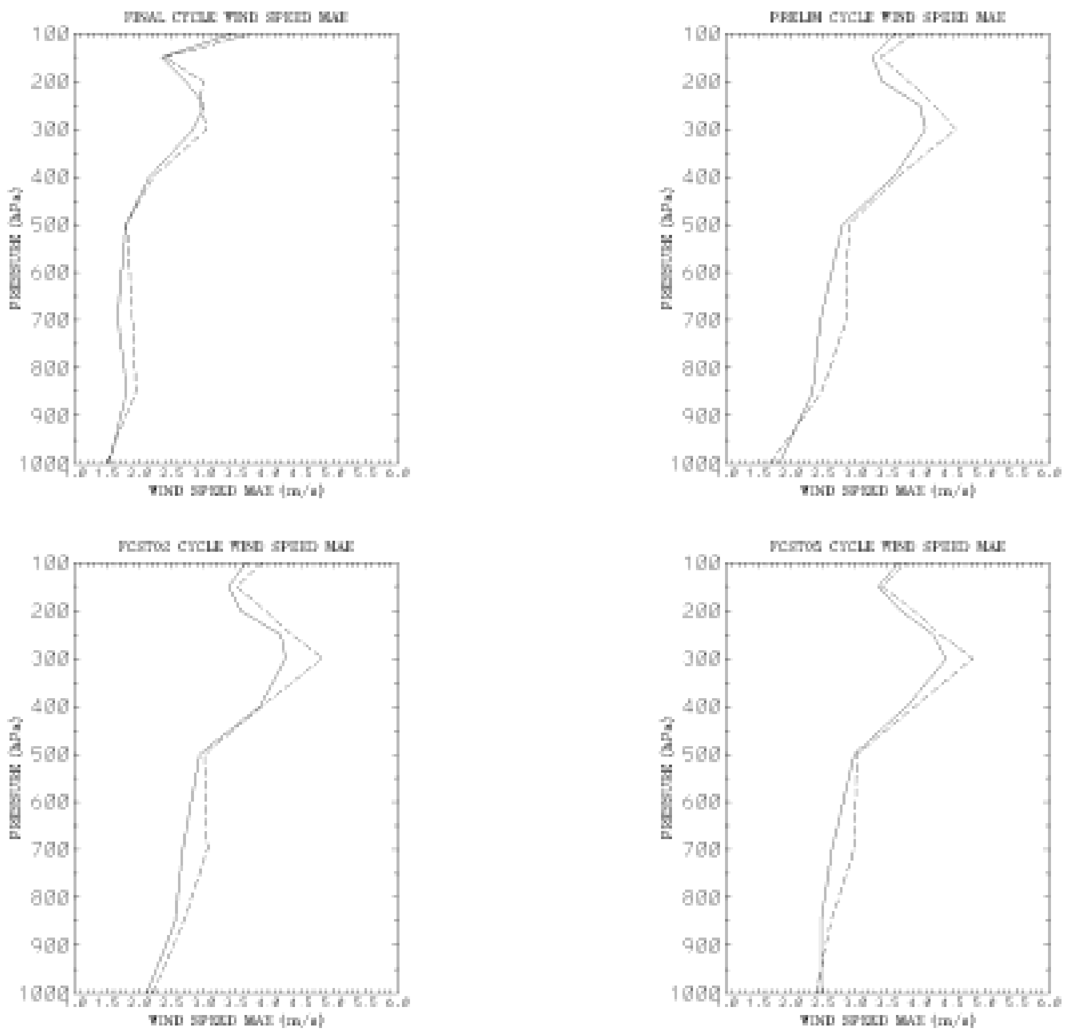

Fig. 5. Mean absolute error (MAE) for wind speed (m/s) calculated for the SAT and NOSAT systems (final, prelim, 2 hr forecast, and 5 hr forecasts) against the 0000 and 1200 UTC rawinsonde observations, over the period from 2001040100 through 2001040712. The solid line is the SAT system and the dashed line is the NOSAT system. The panels shown are for a) final stages valid at 0000 and 1200 UTC; prelim stages available at 0000 and 1200 UTC; c) 2 hr forecasts valid at 0000 and 1200 UTC; and d) 5 hr forecasts valid at 0000 and 1200 UTC.